Chemically Dependent Transport in a Cross-linked H_{II} Phase Lyotropic Liquid Crystal Membrane

Benjamin J. Coscia Michael R. Shirts

March 25, 2019

1 Introduction

We need highly selective and permeable membranes in order to perform efficient separations.

- Cleanup of fracking water
- Removal of organic micropollutants, such as pesticides, pharmaceuticals, and personal care products, from the drinking water supply.
- Desalination
- All of these separations are possible with current commercial membrane separation techniques but they are too energy intensive to be worth the capital investment needed to start the processes.

Nanostructured membranes offer the potential for molecular-level design which could overcome the limitations faced by conventional membrane technologies.

- Mitigation of stochastic aspects of membrane synthesis
- Well-defined and uniform pores increase selectivity
- Solute-specific separations.

H_{II} phase lyotropic liquid crystals have densely packed, uniform sized pores and have the potential to disrupt conventional membrane separation techniques by being selective based not only on solute size and charge, but on chemical functionality as well.

- Uniform pores lead to high selectivity
- The hexagonal geometry is ideal for high permeability

While H_{II} membranes have been synthesized and characterized in a lab setting, there is a limit to the level of detail that can be obtained from experiment.

- The separation performance of these membranes has been primarily characterized with size-exclusion experiments which emphasizes selectivity based on the ability to enter a given pore.
- While size-exclusion is a useful separation, it cannot reliably purify a solution where the solute size is on the same order as water.
- Therefore, it is important to take advantage of material properties other than pore size.
- Unfortunately, the complexity of LLC Membranes has obscured the interpretation of experimental transport studies.

Molecular dyanmics (MD) simulation can give us mechanistic insights with atomistic resolution so that we can directly observe small solute transport within LLC membrane nanopores and intelligently design new membranes for solute-specific separations.

In our previous work, we determined the most likely structure of the hexagonal phase formed by the monomer Na-GA3C11.

- We developed techniques for equilibrating the hexagonal phase made by neat monomer as well as with varying amounts of water in the pores.

In this work, we have studied the transport mechanisms exhibited by a number of polar solutes with varying size, chemical functionality and hydrophilic character.

- Many of the separations we are interested in involve polar organic compounds.

First, we will comment on the membrane's structure.

- We have previously studied dry membrane systems and some systems with low water content.
- We will observe how the radial density of monomer components and water change based on membrane water content.

Then we will present our efforts to understand how small molecules, including water partition within the pores?

- From a macroscopic perspective, it is straightforward to hypothesize that the water and polar solutes spend their time exclusively in the tube-like hydrophilic pore region.
- Our previous work showed that there is a gradual compositional transition from the hydrophilic to the hydrophobic region which means that solutes may not necessarily stay confined to the centers of the pores or even within the pore region.
- We will study the gradient in composition of solutes and water and any resultant influence it might have on mechanistic properties.

Finally, and for the bulk of this work, we will present our observations and explantions of the various transport mechanisms exhibited by water and solutes.

- Given that the pores will restrict motion of the solutes, we anticipate that transport will be hindered in some way.
- We want to understand the differences in solute motion, specifically its mean squared displacement (MSD), based on a solute's size, shape and chemical functionality.
- We will study the interactions between solutes, the membrane, and water in order to determine which mechanism or mechanisms dominate.

There are also a number of questions this study is not intended to answer.

- We will not study the concentration dependence of the observed transport rates. Although the average MSD might change with concentration, we are focused on the underlying solute-membrane interactions that lead to the observed transport mechanisms which we conjecture will be the same regardless of concentration.
- We will not study the chemical potential of solutes in the pores, which could give us a better understanding of equilibrium solute partitioning. This information will not greatly enhance our understanding of mechanistic details in various membrane regions.
- Both of the above points will add unnecessary levels of complexity which can be left for a future study.
- This work is a simple starting point meant for observing the types of interactions which occur between isolated solutes and the membrane.

2 Methods

Python scripts used to set up systems and conduct post-simulation trajectory analysis are available online at `https://github.com/shirtsgroup/LLC_Membranes`. The appropriate script to use for each of the following calculations is summarized in Table S1 of the SI.
We ran all molecular dynamics simulations and energy minimizations using GROMACS 2018.3 [1, 2, 3, 4]

System Setup

Stable H_{II} phases, assembled with Na-GA3C11, can be formed using a broad range of water concentrations.

- In the literature, this system is typically synthesized with close to 10 wt % water [5, 6]
- However, Resel et al. noted that the system is likely fully hydrated with less than 7 wt % water. [7]
- We decided to test two different levels of water content: 5 and 10 wt %

We observed that water partitions into the tail region of our system and therefore built our initial configurations with water in both regions close to the expected equilibrium value.

- We define the partition between the pore and tail region to be ca. 1.5 nm from the pore center based on the minimum in the radial distribution of water (See section 2).
- The amount of water present in the tails may or may not be experimentally consistent but if we don't put it in, the results will not be thermodynamically consistent, which will give issues with measurements and calculations.
- We iteratively adjusted the pore radius in our systems until the right amount of water fit in the pores when we ran `gmx solvate`.
- We placed water molecules in the tail region one at a time in random locations with short energy minimizations between insertions.
- When studying transport of water in the pores, we limited the calculations to water molecules that spend greater than 95 % of their time in the pore region.

We equilibrated an initial solvated configuration before adding solutes.

- First, we equilibrated the initial configuration using the 'wet' equilibration procedure described in our previous work [8].
- Then we cross-linked the equilibrated solvated configuration using the cross-linking procedure described in our previous work.

To study a given solute, we added 6 solute molecules to each pore of the equilibrated cross-linked configuration.

- We equally spaced each solute in the pore
- 6 solutes per pore provided a balance of a useful amount of data for generating statistics and a low degree of interaction between solutes (reference to supporting information to show low degree of interaction)
- At each insertion point we placed a randomly oriented solute molecule then ran a short energy minimization.
- We allowed the solutes to equilibrate for 5 ns using berendsen pressure control
- We collected transport data over the course of 1 μs MD simulations

Solute Parameterization

Like we have previously done for Na-GA3C11 [8], we parameterized the interaction potential for the solutes using the Generalized AMBER Force Field (GAFF) [9] with the Antechamber package [10] provided with AmberTools16 [11]. We chose GAFF because it has been parameterized for use with organic molecules. We assigned atomic charges using the am1bccsym method of `molcharge` shipped with QUACPAC from Openeye Scientific Software.

Mean Squared Displacement

We measured the time-averaged z-direction mean squared displacement (MSD) of the centers of mass of each solute over the course of 1 μs MD simulations using Equation 1.

- $$\overline{x^2(\tau)} = \frac{1}{T-\tau}\int_0^{T-\tau}(x(t+\tau)-x(t))^2 dt \tag{1}$$

  where τ is the time lag and T is the length of the trajectory [12].

- Generally, the MSD grows according to Equation 2,

$$\langle x^2(t)\rangle = K_\alpha t^\alpha \tag{2}$$

- where α is the anomalous exponent and K_α is the generalized diffusion coefficient.
- A value of $\alpha < 1$ indicates a subdiffusive process, while a value of $\alpha = 1$ and $\alpha > 1$ is characteristic of Brownian and superdiffusive motion respectively.
- In practice, α corresponds to the growth of the *ensemble* MSD given by Equation 3 [12]:

$$\langle x^2(t)\rangle = \langle x(t) - x(0)\rangle \tag{3}$$

- The ensemble MSD is calculated with respect to a reference position and hence carries some dependence on its starting point.
- The time-averaged MSD averages over all possible time lags of a given length, effectively eliminating any initial configuration dependence and generating an increased number of observations.
- For ergodic systems, both types of MSDs will be equal.
- Since we have a small number of solutes with which to generate statistics and because we are not calculating values for α in this particular study, we will only use the time-averaged MSD.

We fixed the length of each simulated trajectory so that we could compare the total MSD between different solutes without the influence of the ageing phenomenon.

- Ageing is defined by the tendency of the average slope of an MSD curve to decrease as the length of trajectories are increased [13].
- The maximum measured dwell time can be no longer than the total length of a simulated trajectory.
- As measurement time or trajectory length is increased, longer dwell times are incorporated into the calculation, lowering the average MSD.
- Because the MSDs are non-linear and because of the ageing phenomenon, we did not attempt to calculate a diffusion constant as one might for a Brownian particle with a linear MSD.
- Instead, the reported values for MSD represent the average MSD for a given solute after a 400 ns time lag.

Molecular Size Determination

In order to determine an effective radius for each solute, we measured the maximum pairwise distance between atoms of each solute over the course of a 2.5 ns simulation of solutes dissolved in a cubic box of water.

- Each box consisted of about 2100 water molecules and 6 solutes.
- Although there exist more involved methods for determining the hydrodynamic radius [14], we chose to use a simpler and more intuitive metric since we are only interested in observing trends in the solute mean squared displacement as a function of solute size.

The Stokes-Einstein Relationship

The Stokes-Einstein relationship expresses the diffusion coefficient of a hard spherical particle as a function that is inversely related to the particle's radius:

- $D = \dfrac{k_b T}{6\pi\eta r}$
- where k_b and T are the Boltzmann constant and the system temperature respectively and η is the system's viscosity.
- For the largely demonstrative calculations relevant to this study, we assume that the system viscosity is constant since we only make minor changes to the membrane's composition and accurately assessing the viscosity in a complex and inhomogeneous system such as ours is a challenge by itself.
- Additionally, rather than calculate D, we will apply the relationship to analyze solute MSDs, which is valid because all trajectories are of the same length.

It is well-known that the relationship breaks down when solute size becomes on the order of solvent size because the solute can no longer be treated as a non-interacting hard sphere.

- Gierer and Wirtz introduced a microfriction correction factor in order to address this issue.
- They proposed that $D = \dfrac{k_b T}{6\pi\eta f r}$
- Where $f = \left(1.5(r_2/r_1) + \dfrac{1}{1 + (r_2/r_1)}\right)^{-1}$
- and r_1 and r_2 are the radii of the solute and solvent molecules respectively.

Radial Distribution Functions

We measured the average radial distance of each solute of interest from the pore centers.

- We binned the radial distances and then normalized by the volume of the annulus defined by the bin edges.
- Although the pores are often described as straight, they have a small degree of tortuosity which disrupts the RDF calcuation.
- We tried to mitigate the effects of tortuosity by calculating the RDF with respect to splines that run through the pore centers.
- Each spline consists of 10 points, equally spaced in the z-direction, whose (x, y) coordinates are defined based on the center of mass of all head groups closest, in z, to the given point.
- When calculating RDFs, the radial distance from the pore center is based on the distance between the solute center-of-mass and the linearly interpolated (x, y) coordinates of the pore center calculated based on the spline.

- Using the splines, we calculated the tortuosity of the pores by calculating the ratio $\frac{L}{Z}$ where L is the length of the spline and Z is the length of the unit cell in the z-direction.
- The average tortuosity of each pore is 1.03 ± 0.01 and 1.07 ± 0.02 in the 5 and 10 wt % systems respectively.

In all RDF plots, we include the average RDF of the head groups as a reference.

- The head group RDF shown is the average of the head group RDFs for each solute system in the plot.
- We generated 95 % confidence intervals by bootstrapping the frame-by-frame RDFs obtained from both systems.

Identification of Hydrogen Bonds

Based on the geometric criteria proposed by Luzar and Chandler [15], we determined a hydrogen bond to exist if the distance between the donor, D, and acceptor, A, atoms is less than 3.5 Å and the angle formed by D–H...A is less than 30°.

- Attempts to describe a hydrogen bond in the context of molecular simulations has yielded a number of definitions with no true consensus [16].
- The geometry of hydrogen bonds has some dependence on the system being studied.
- The definition of Luzar and Chandler is easily visualized for trajectories using the `hbonds` representation of the Visual Molecular Dynamics (VMD) software package which allows us to directly check the validity of identified hydrogen bonds.
- In section S2.3 of the SI, we show that our conclusions are insensitive to this definition within a reasonable range.

Coordination number

We quantified the coordination of solute constituent atoms with sodium ions.

- For each frame, we counted the number of coordinated molecules to a given solute atom based on a distance cut-off.
- Using four different methods, Rowley and Roux observed peaks in the radial distribution function for sodium coordinated with water at an O-Na distance of between 2.3 and 2.5 Å [17].
- We used 2.5 Å as the distance cutoff.
- We found that this approach is more useful than calculating the 3D spherical radial distribution function because it gives detailed frame-by-frame information rather than an average.

Using our procedure we found that sodium ions in a solution of tip3p water coordinate with an average of 3.6 water molecules.

- We created a 4 x 4 x 4 nm cubic box of water with the GROMACS tool, `gmx solvate`
- We used `gmx genion` to replace water molecules with sodium and chloride ions in order to create a 0.1 M NaCl solution.
- We let the system simulate for 5 ns and reported the average number of coordinated water molecules per frame after discarding the first ns of simulation.

3 Results and Discussion

Structure of Membrane Constituents

Before beginning the analysis of transport behavior, it is important to elucidate the topology of the membrane pores.

In contrast to our previous work with a solvent-free version of this membrane, the pore region of the 5 and 10 wt % water systems are primarily filled with water and sodium ions.

- In dry systems, the pore center is densely filled with sodium ions and head groups (See Ref [8]).
- Figure 1 plots the densities of each membrane constituent in the 5 and 10 wt % systems.
- Water is densest at the center of each pore.
- Sodium ions are densest between the pore center and the peak head group density (black dashed line).
- The peak density of sodium ions is not at the pore center in either case likely because they are still loosely associated with the monomer's carboxylate head groups.

Pores in the 10 wt% water system are wider and less crowded by monomers than those in the 5 wt% water system.

- The peak head group density of 10 wt% water systems is about 0.2 nm further from the pore center than the 5 wt%
- The 5 wt % water system has a non-negligible amount of tail group atoms that occupy the pore center.
- Based on these observations, we expect solute transport to be fastest in the 10 wt % system.

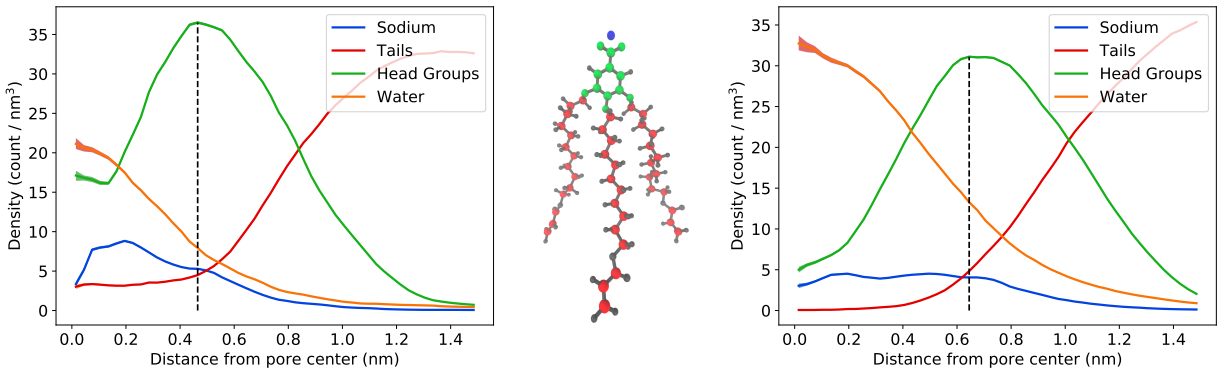

(a) 5 wt% water

(b) 10 wt% water

Figure 1: The radial densities of various monomer components paint a picture of the pore topology where the pore centers are primarily composed of water and sodium ions. All RDFs represent the number of atoms located at a given distance from the pore center normalized by the volume of the annular bin to which they belong. The pores of the 5 wt % system (a) appears to be much more crowded by monomers than the 10 wt % system (b). Head groups in (a) are densest about 0.2 nm closer to the pore center than in (b). A small amount of tail components find their way close to the pore center of the 5 wt % system.

There is an appreciable amount of water that partitions into the tail region of both systems.

- 28 % and 31 % of the total water is present in the tail regions of the 5 and 10 wt% water systems respectively
- See section S2 of the SI for more details.
- This result is likely due to a combination of the lower density of the tail region and oxygen atoms at the ends of each monomer tail which can stabilize water molecules.

Mechanisms Governing Small Solute Transport

We observed transport of sodium, water and 20 other small polar solutes inside the membrane nanopores.

- First, we will comment on transport of the membrane constituents, water and sodium, in a system absent of any additional solutes.
- Then we will present the general trends that we observe among the set of solutes studied.

Water and Sodium Ions

Water's mobility is increased when pores are larger and less crowded.

- The MSD of water is about 65 times higher and the MSD of sodium is about 40 times higher in the 10 wt% system.
- Water moves about 65 times faster than sodium in the 10 wt % system and 40 times faster than sodium in the 5 wt % system.
- The diffusivity of water in the 10 wt % system is still only 1 % that of bulk water

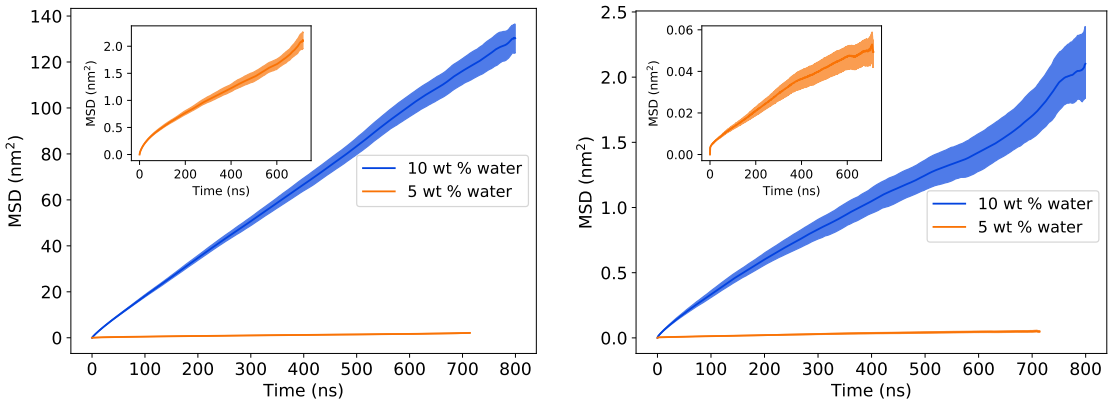

(a) Water

(b) Sodium Ions

Figure 2: (a) The MSD of water in the 10 wt % water system is about 65 times higher than water in the 5 wt % water system. (b) The MSD of sodium in the 10 wt % water system is about 40 times higher than sodium in the 5 wt % water system.

Sodium coordinates with far less water molecules than it does in bulk solution.

- Compared to 3.4 coordinated water molecules in bulk solution (see section 2), sodium ions in our system are, on average, coordinated to about 1.7 water molecules in the 10 wt % system and 1.2 water molecules in the 5 wt% system.
- However, the sodium ions are not undercoordinated since they frequently pair with carboxylate head groups.
- On average, sodium ions coordinate with 0.5 carboxylate group oxygen atoms in the 10 wt % water system and 0.4 carboxylate oxygen atoms in the 5 wt % water system.

Transport of Small Polar Solutes

We observe trends in transport properties that are dependent on chemical environment within the nanopores as well as the chemical functionality of membrane constituents rather than just solute size.

- Polar solutes are slowed by interactions between monomer functional groups and ions.

- Solutes with hydrophobic character partition out of the pore and are slowed by densely packed organic monomer components.
- A thorough understanding of these interactions will help us to create monomer design principles.
- We will begin our analysis by considering the collective trends observed across all systems and then focus on subsets of similar molecules where some exceptions occur.

Like water and sodium above, the MSDs of the solutes studied in this work are significantly larger in the 10 wt % system, than those in the 5 wt % water system (Figure 3).

- The fastest moving solute in both cases, methanol, has an MSD about 175 times larger in the 10 wt % versus the 5 wt % system.
- Clearly the equilibrium water content of a given LLC system will determine its viability for real separations.

The MSDs depend on more than just solute size.

- We plotted the solute size against their MSDs in Figure 3c and 3d.
- Assuming that the Stokes-Einstein relationship is no longer valid for solutes with a radius less than x nm, we fit the Stokes-Einstein relationship with and without the correction factor making sure that the two curves intersected at x nm and that the corrected line passed through the highest MSD data point, methanol.
- We believe methanol is subject to the least hindrance due its small size and relatively fast motion.
- Although both curves are approximations, they illustrate that the majority of solutes in our study show lower than expected MSDs.
- In most cases, the predicted MSDs even fall below the conservative Stokes-Einstein estimate.
- It is clear that more complex mechanisms determine the MSDs of these solutes.

On the timescales simulated in our study, solutes exhibit subdiffusive behavior.

- Figure 4a plots the z-coordinate versus time of 3 representative ethanol centers of mass in the 10 wt % water system.
- There are clear periods of entrapment separated by relatively large hops.
- The MSD calculated based on all ethanol molecules is plotted in Figure 4b and is sublinear.
- The long periods of entrapment likely lead to this sublinear, and thus subdiffusive, behavior.

Solutes partition out of the pore into the head group region and beyond which may lead to radially dependent transport mechanisms.

- It is clear from Figure 4a that the longest periods of entrapment usually occur when solutes are far from the pore center.
- There is a high resistance to movement in the dense head group and tail regions.
- When hops occur, and where there is the most z-positional noise, solutes are generally close to the pore center.
- Solutes can move relatively freely when they enter the pore region which is primarily composed of water molecules and sodium ions.

In addition to solute trapping in dense monomer regions, we observe a second trapping mechanism caused by preferential hydrogen bonding between hydrogen bond donor solutes and monomer head groups.

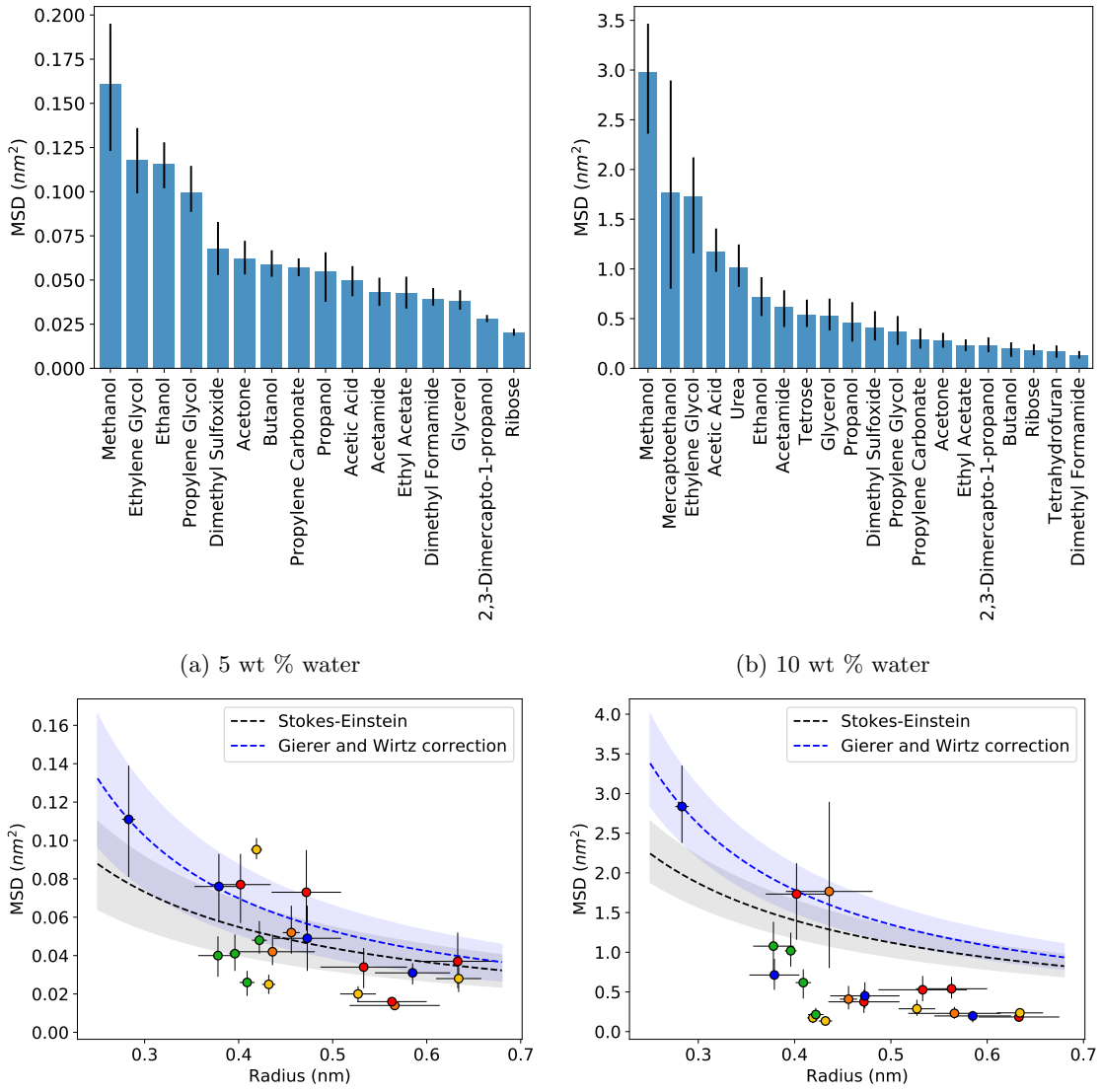

(a) 5 wt % water

(b) 10 wt % water

(c) 5 wt % water

(d) 10 wt % water

Figure 3: The MSDs of solutes in the 5 wt % water system (a) are significantly smaller than those of the solutes in the 10 wt % water system (b). The MSDs are not a monotonic function of molecular size (c and d). A significant number of solute MSDs fall below the theoretical lines predicted by the Stokes-Einstein equation and Gierer and Wirtz' corrected Stokes-Einstein equation.

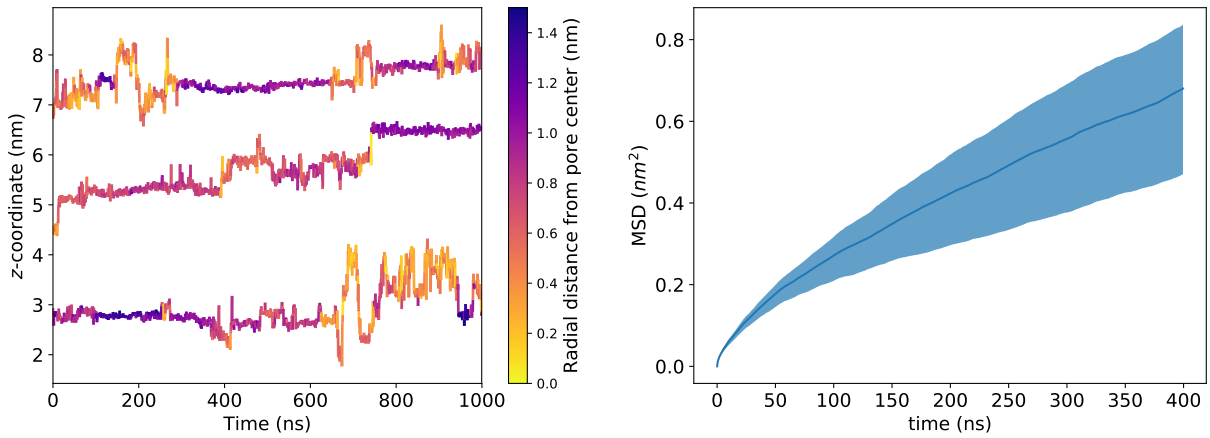

(a) (b)

Figure 4: All solutes show subdiffusive transport behavior inside the membrane's nanopores, similar to that exhibited by ethanol. (a) The z-coordinate trace of 3 representative ethanol COMs shows clear periods of entrapment separated by hops. In general, the longest dwell times occur when solutes are situated far from the pore center and the hops occur when solutes are close to the pore center. (b) The time-averaged MSD of ethanol is not linear which suggests transport is governed by an anomalous subdiffusion process.

- To continue with our ethanol example, we observe that the 24 ethanol molecules donate an average of 15.7 hydrogen bonds per frame and accept 0.6 hydrogen bonds per frame.
- On average, 40 % of hydrogen bonds donated by ethanol go to carboxylate head groups, 25 % go to the ether linkages between the tails and the head groups and the remaining 35 % to water.
- There are less carboxylate oxygen atoms in the pore than there are water molecules yet more hydrogen bonds are donated to them.
- The stability of hydrogen bonds with carboxylate oxygen atoms is likely high since the oxygen atoms have a negative charge with no neutralizing positive charges nearby.
- Additionally, on average, each sodium ion is coordinated to 1.7 water molecules meaning an appreciable fraction of the water molecules occupying the pore region are usually coordinated to a sodium ion which decreases their availability to accept hydrogen bonds from solutes.

Finally, we see instances of solutes that become immobilized or slowed by association with sodium counterions.

- Much like water, the polarity of the solutes creates regions of high electron density, modeled using partial negative charges, which are stabilized through electrostatic interactions with sodium ions.
- There are many cases in which polar groups bind to sodium ions for at least a short period of time.
- Some kind of pair time distribution

The transport behavior exhibited by solutes in the 5 wt % water systems is similar to that shown by those in the 10 wt % system however the timescales are much longer.

- We observe subdiffusive behavior with intermittent hopping between periods of entrapment.
- The frequency and length of hops are both diminished in the 5 wt % system.
- Since there are only 24 solute molecules in each system, in order to obtain better time-averaged descriptions of solute transport mechanisms, we will focus the rest of our analysis on transport in the 10 wt % water systems.

Transport of Simple Alcohols

The MSDs of methanol, ethanol, propanol and butanol descend in order of their size.

- Using methanol as a reference, the other alcohols move slower than expected according to both the pure Stokes-Einstein relationship and the corrected relationship (See Figure 5a).

Methanol moves fast, not only because it is the smallest solute studied in this work, but because it has the highest radial density near the pore center where the largest hops occur.

- The radial density as a function of distance from the pore center for each alcohol is plotted in Figure 5b.
- On average, the density of methanol in the pore center is only slightly less than the density near the head groups.
- All other alcohol molecules are most concentrated in the head group region.

All simple alcohols participate in a similar number of hydrogen bonding interactions with the monomer head groups, but with varying preference towards hydrogen bonds with the monomer carboxylate oxygen atoms over the ether oxygen atoms (See Figure 5c)

- If all 5 hydrogen bonding acceptor sites on the monomer head groups were equal, we would expect the ratio of the number of hydrogen bonds between solutes and the two carboxylate oxygen atoms to the number of hydrogen bonds between solutes and the three ether groups to be 2/3.
- There is a clear preference towards hydrogen bonding with the carboxylate oxygen atoms for all simple alcohols.
- This is largely due to the large net charge of the carboxylate groups as well as the more highly crowded environment surrounding the ether oxygen atoms.
- Butanol shows the largest preference towards hydrogen bonds with carboxylate head groups.
- The radial distribution function of atoms located at opposite ends of butanol shows that, on average, oxygen atoms are situated 0.25 nm closer to the pore centers than the distal carbon atoms.
- This suggests that alcohols tend to orient themselves like the liquid crystal monomers, with hydrophilic components point towards the pore centers.

Transport of Diols, Triols and Sugars

The order of the MSDs of solutes in this grouping are roughly consistent with their size, however propylene glycol moves exceptionally slow.

- Ethylene glycol has the highest MSD followed by tetrose and glycerol, whose MSDs are similar, propylene glycol, the second smallest solute of this set, and finally ribose.

Transport is both facilitated and hindered by additional solute hydroxyl groups due to their influence on radial density and hydrogen bond frequency.

- Extra hydroxyl groups cause solutes to favor the water-rich pore region. where there is the least hindrance to movement (See Figure 6b).
- Tetrose, ribose and glycerol are densest close to the pore center. This is likely a consequence of both their hydrophilicity and large size which prevents them from partitioning into the head group region.
- However, these extra hydroxyl groups facilitate a larger number of hydrogen bond interactions that work to hold solutes in place (See Figure 6).
- It has been observed that hydrogen bonding in a system will generally reduce diffusivity [18]

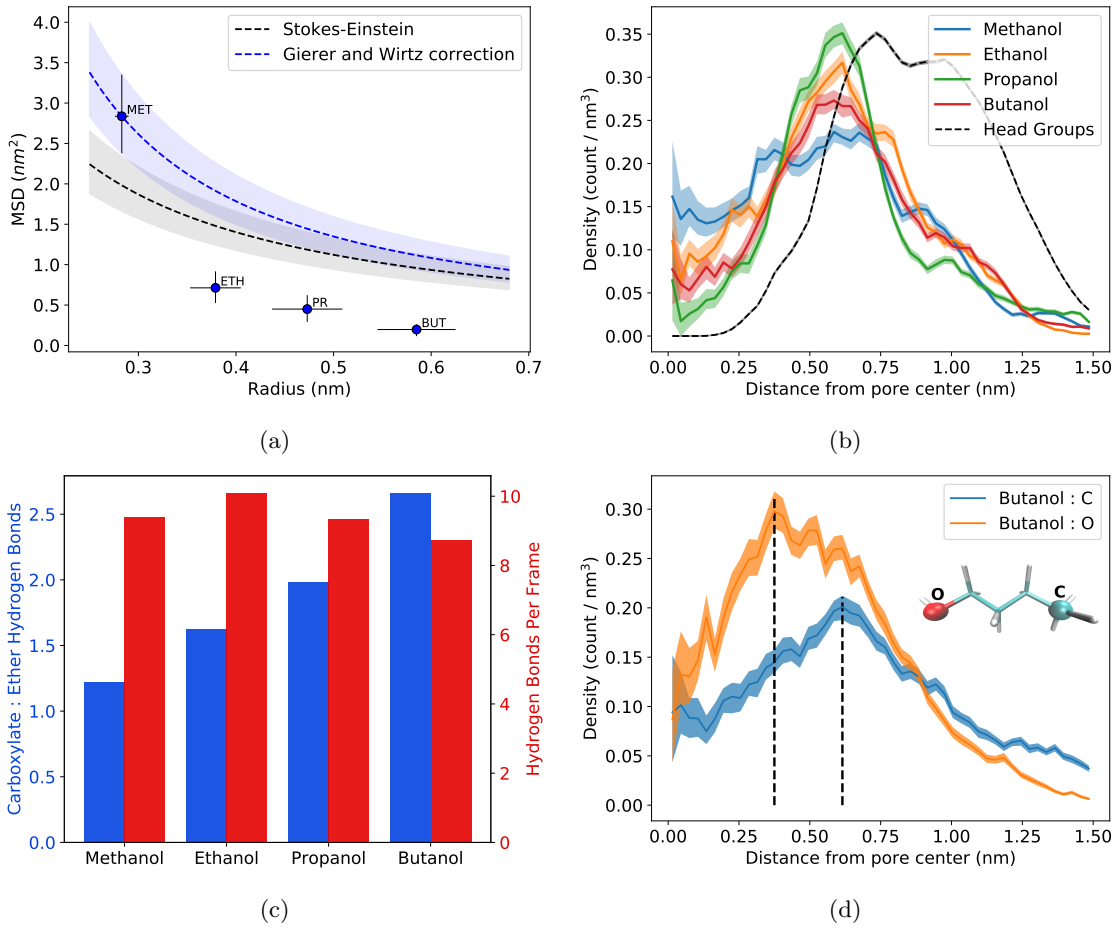

Figure 5: (a) The MSD of the simple alcohols decrease as a function of the solute size, however methanol's MSD is considerably higher than expected based on the Stokes-Einstein equation. (b) The radial distribution functions of each simple alcohol shows a maximum close to the highest density of monomer head groups (dashed line, normalized for easier visual comparison). Methanol spends the largest proportion of time, relative to the other alcohols, near the pore center, which may help explain its fast dynamics. (c) Despite relatively little difference in the total number of active hydrogen bonds per frame, a given alcohol's preference towards hydrogen bonds with the carboxylate groups increases with molecule size. (d) The average location of butanol's oxygen atom is significantly closer to the pore center than its most distal carbon atom, suggesting that the molecule is oriented with hydrophobic tails pointing away from the pore center.

The number of hydrogen bonding interactions between solutes and head groups increases with the number of solute hydroxyl groups.

- These solutes frequently undergo simultaneous hydrogen bond interactions as shown in Figure 6.
- For example, both hydroxyl groups of ethylene glycol can undergo hydrogen bonds with different hydrogen bond acceptors at the same time.
- In some cases, all 4 hydroxyl groups of ribose hydrogen bonded to monomer head groups simultaneously.
- Hydrogen bonds act as a kind of molecular glue which holds solutes in place, especially when there are many, however proximity to the pore center partially compensates for this effect in the cases of glycerol and tetrose, causing them to have relatively high MSDs for their size.

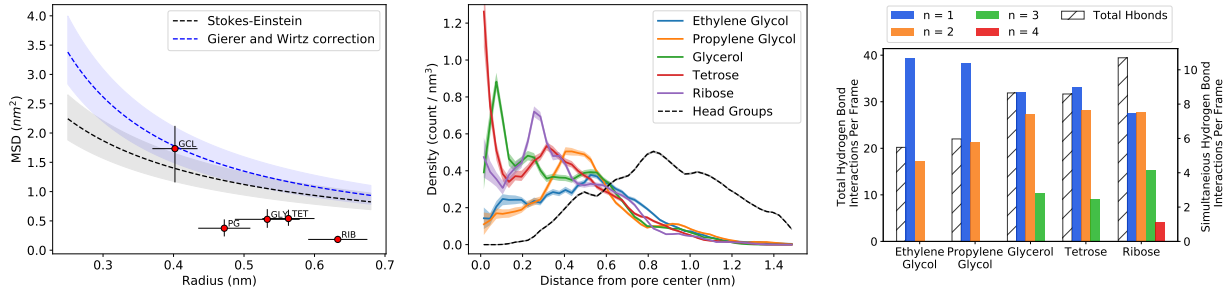

(a) (b) (c)

Figure 6: (a) Glycerol, tetrose and ribose are densest close to the pore center because they have a high number of hydrophilic groups and are relatively large. Ethylene glycol and propylene glycol are densest close to the head group region. (b) The number of hydrogen bond interactions between solutes and monomers increases as solutes gain additional hydroxyl groups. The number of hydrogen bonds made by a single solute in different locations simultaneously, n, also increases with the number of hydroxyl groups. In the most extreme case, all four hydroxyl groups of Ribose (n = 4) are involved in a hydrogen bond interaction at the same time.

Of the two diols, ethylene glycol moves significantly faster than propylene glycol due to propylene glycol's affinity for the monomer head groups.

- Combined with an increase in size, the addition of a single methyl group to ethylene glycol increases propylene glycol's hydrophobic character and causes it to favor positions near monomer head groups.
- Both diols have comparable densities close to the pore center, however propylene glycol's density has a large peak near the monomer head groups relative to ethylene glycol.
- Propylene glycol can form more highly stabilized hydrogen bonds with carboxylate groups, explaining the higher incidence of hydrogen bonds shown in Figure 6.
- Somewhat counterintuitively, there is a relatively high density of ethylene glycol molecules beyond the head group region probably due to its relatively small size. This likely contributes to the somewhat large error bars on its MSD in Figure 3.
- This implies that hops performed by ethylene glycol must be considerably larger than those by propylene glycol in order to result in consistently larger MSD values.

Transport of Ketones and Amides

The 4 ketone-like molecules tested show a surprising range of transport behaviors.

- Urea, acetic acid, acetamide and acetone are all characterized by a carbonyl group with two attached heavy atoms.
- All are similar in size and are planar molecules due to the sp2 hybridization of their carbonyl group.
- The fastest solutes of this grouping, acetic acid and urea, are about 3 times faster than the slowest, acetone.

The MSD of the solutes descend in order of their density close to the pore center.

- As shown in the radial density functions (Figure 7b), Acetic acid has a fairly uniform and high density within the pore region.
- Acetone spends relatively little time near the pore center with its peak density nearest the peak head group density.

The amides, urea and acetamide, hydrogen bond with head groups relatively infrequently, but regularly coordinate with sodium ions (See Figure 7).

- In an average frame, acetic acid participates in more than 12 hydrogen bonds with monomer head groups while urea and acetamide participate in less than 2.
- Urea and Acetamide both have hydrogen bond donating nitrogen atoms, however nitrogen is a weaker hydrogen bond donor than oxygen due to its lower electronegativity.
- Given their lower propensity to hydrogen bond one might expect amides to partition out of the pore and/or to move through the pore quickly, perhaps faster than methanol.
- Both RDFs contain peaks in their radial density that are situated between the pore center and the head groups, but closer to the pore center than other solutes that hydrogen bond with carboxylate groups.
- Solutes that hydrogen bond frequently tend to show peaks in their RDFs near 0.5-0.6 nm from the pore center (see Figure 5b, for example) and those that coordinate with sodium ions more frequently tend to show peaks in their RDFs near 0.2-0.3 nm from the pore center.
- Both solutes spend about half of their time with their carbonyl oxygen atom coordinated to a sodium ion which restrains the solutes to within the pore region
- Only the carbonyl oxygen atoms coordinate with sodium ions. The nitrogen atoms do not coordinate at all despite a similar negative partial charge because the attached hydrogen atoms shield this interaction by making the NH_2 group approximately neutral.

Acetone has the lowest MSD of this set because it either coordinates with sodium or stays trapped near and behind the head groups.

- On average, acetone coordinates with sodium with the same frequency as acetic acid which is manifested as a peak in its RDF about 0.2 nm from the pore center.
- However, acetic acid spends more time in the pore center and therefore encounters more sodium ions.
- When an acetone molecule coordinates with a sodium ion, its polarity is largely neutralized and it retreats towards the head group region where it can easily get trapped.
- Acetic acid and the amides have other, unoccupied, hydrophilic groups while bound to sodium ions which increases their stability in the pore.

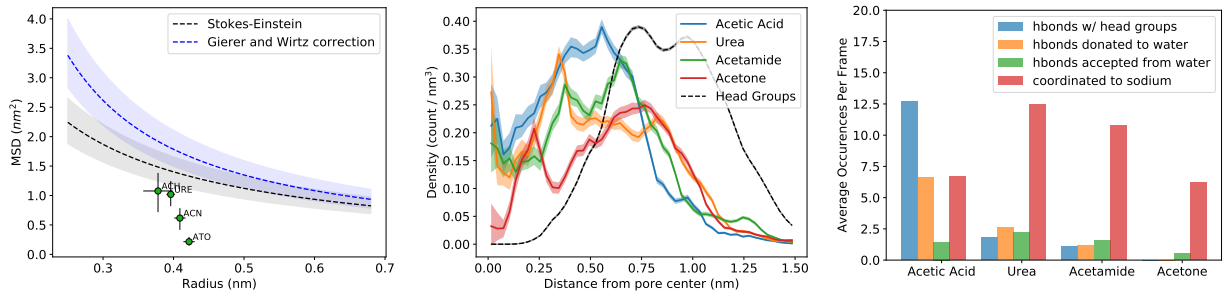

(a) (b) (c)

Figure 7: (a) The radial density near the pore center (r = 0) decreases with decreasing solute MSD. Peaks in the RDFs of urea, acetamide and acetone near 0.2 - 0.3 nm from the pore center are likely due to coordination with sodium ions. (b) The amides hydrogen bond with water far less than acetic acid, however they tend to coordinate with sodium ions more frequently.

Transport of Thiols

We also studied the transport properties of sulfur analogs of glycerol, ethylene glycol and acetone.

- We replaced all but one oxygen atom of ethylene glycol and glycerol with sulfur atoms to create dimercaptoethanol and 2,3-dimercapto-1-propanol.
- We replaced the carbonyl carbon of acetone with sulfur in order to create DMSO.
- Sulfur is unable to hydrogen bond making thiols less soluble in water than their hydroxyl group analogs.

Mercaptoethanol has a similar average MSD and RDF to ethylene glycol.

- There is a much larger uncertainty associated with mercaptoethanol's MSD.
- Some of this can be accounted for by the higher density of mercaptoethanol molecules in the head group / tail region, where transport is inherently slower.
- There are nearly 40 % more mercaptoethanol molecules than ethylene glycol molecules beyond 0.8 nm from the pore center.
- It hydrogen bonds with head groups 6 times less frequently than ethylene glycol. which may lead to larger hops when in the pore region.
- The range of behaviors shown by mercaptoethanol explain the large variance of its MSD.
- Average hop length while in pore region maybe

2,3-dimercapto-1-propanol exhibits slower transport than glycerol because more of it partitions into the tail region.

- The density of glycerol is always higher up to 0.7 nm from the pore center where the population of 2,3-dimercapto-1-propanol then becomes more dense into the tail region.
- Glycerol participates in about 3 times as many hydrogen bonds as 2,3-dimercapto-1-propanol.
- Because sulfur cannot hydrogen bond, 2,3-dimercapto-1-propanol is less soluble than glycerol in the water-filled pores and more readily partitions into the tail region.

DMSO has a comparable if not larger MSD than acetone even though it is a slightly larger molecule.

- The density of DMSO is higher than acetone in the pore region, except for the peak exhibited by acetone near 0.2 nm, which is due to sodium ion association.

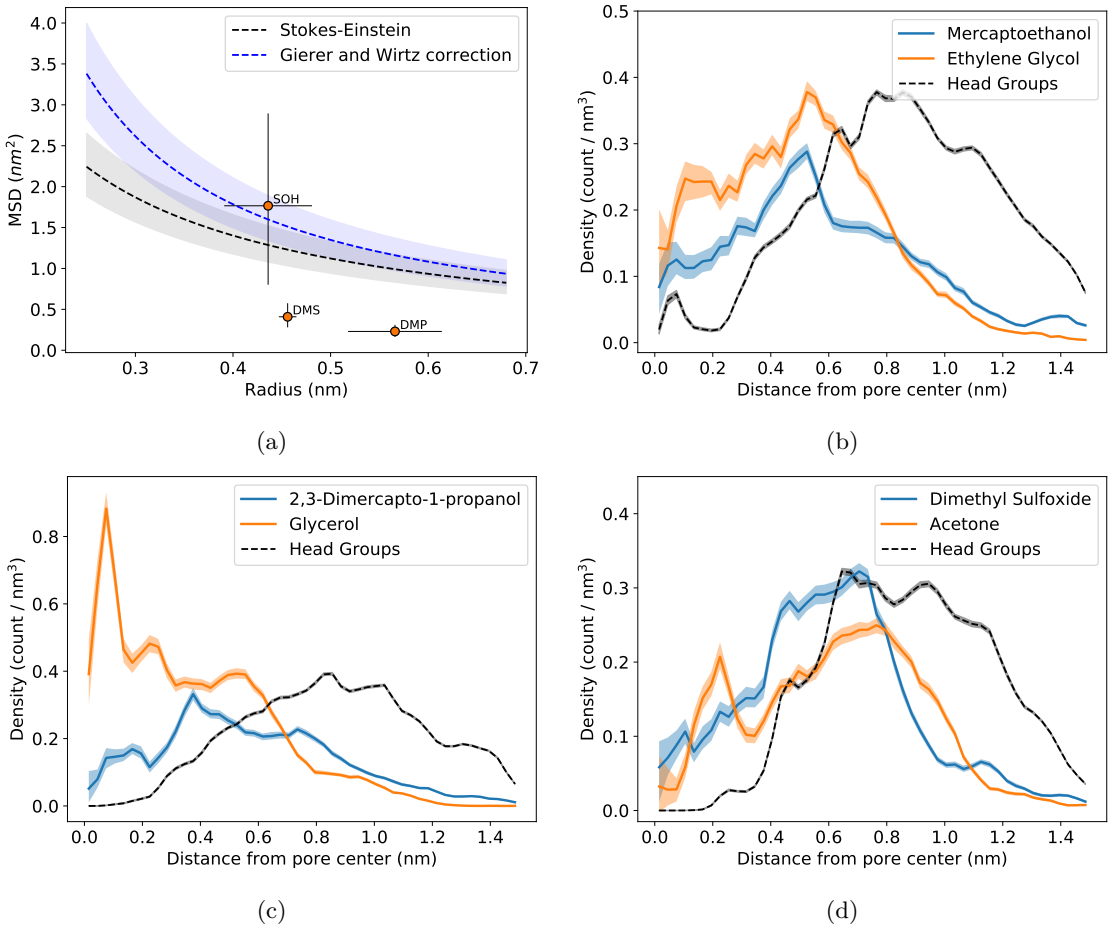

Figure 8: (a) The RDF of mercaptoethanol is similar to ethylene glycol except for its higher density in the tail region and consequently lower density in the pore region. (b) 2,3-dimercapto-1-propanol is densest near the head groups, unlike glycerol whose density is very high close to the pore center. (c) Overall, dimethylsulfoxide has a higher density than acetone within the pore region which may in part explain its marginally larger MSD.

- On average, 35 % of DMSO molecules are coordinated to a sodium ion each frame compared with 26 % of acetone molecules.
- The pyramidal structure of DMSO may force it to spend more time closer to the pore center which increases its interaction with sodium ions.
- The tendency of DMSO to stay in the pore region counterbalances the sodium ion interactions to give it a higher MSD than acetone.

Hydrogen Bond Acceptors

The slowest set of molecules we studied can accept hydrogen bonds, but cannot donate them.

- Among this set are the two slowest solutes in our study: Tetrahydrofuran and Dimethyl Formamide.
- The MSDs of ethyl acetate, propylene carbonate and acetone are only marginally larger.

The radial density of solutes near the pore center in this set is surprisingly high as shown in Figure 9b.

- Propylene carbonate and ethyl acetate are among the largest solutes in this study. Their size prevents them from easily entering the tail region and consequently gives faster transport properties
- However, this is not a hard rule. When a solute does overcome the barrier of entry beyond the head group region, it can become trapped. All solutes in this set show at least a small peak ≥ 0.9 nm from the pore center which is likely caused by solutes that get trapped in the tail region for a significant amount of time.

Solutes do not make frequent hops while in the pore region.

- DMF experiences a similar effect, but to a lesser extent. Its density is higher than THF near the head groups. The planar shape of DMF causes it to become stuck between head groups. Excursions into the pore region do not necessarily result in large hops.

Carbonyl groups continue to show high degrees of association with sodium ions.

- The number of sodium ions coordinated to the carbonyl group of propylene carbonate, dimethyl formamide, ethyl acetate are consistent with that shown by acetone, all between 6 and 7 per frame (See figure 9c)
- The carbonyl group of the amides studied in the previous section associate with sodium nearly twice as frequently as compounds that don't contain nitrogen (see figure 7c).

4 Conclusion

We have examined the transport characteristics of a series of small polar molecules in our model of the H_{II} phase formed by the liquid crystal monomer Na-GA3C11.

We learned that the MSD of solutes, water and counter ions are highly dependent on LLC membrane water content.

- The MSD of these components is about 2 orders of magnitude larger in the 10 wt % system than the 5 wt % system.
- As more water is added to the system, the pores become less crowded with monomer components
- The amount of water in the pores deserves special attention when screening new monomers.

We observed three mechanisms of solute entrapment.

- A solute can become stuck among monomer tails.

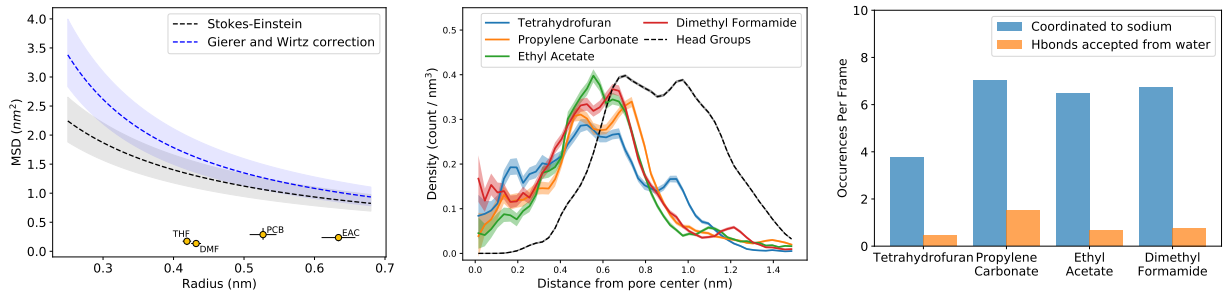

(a) (b) (c)

Figure 9: (a) The radial density of solutes that can only receive hydrogen bonds is surprisingly high in the pore region. Conversely, there is also an appreciable amount of each solute in the tails. (b) The low MSDs exhibited by each of these solutes is due to a combination of entrapment within the tail region and a high degree of coordination with sodium ions.

- A solute can donate hydrogen bonds to monomers.
- A solute can associate with a bound counterion.

Based on these trapping mechanisms, we can suggest modifications that can be made to monomers in order to mitigate or enhance their effect on solute MSDs.

- Since solutes move slowly while entangled among the monomer tails, one can try to design monomers that better control the partition of solutes between the pore and tail region.
- For example, removal of the ether linkages between the head groups and the monomer tails will decrease the stability of polar molecules near the head groups.
- Alternatively, one can focus on designing head groups with varying hydrogen bonding capabilities.
- One can increase the number of hydrogen bonding sites on the head groups in order to trap more solutes, or decrease the number of hydrogen bond sites to trap less.
- Finally, one can attempt to control the degree to which solutes coordinate with counterions.
- Changing the size and valence of the counter ion may offer some interesting behavior.

Supporting Information

Detailed explanations and expansions upon the results and procedures mentioned in the main text are described in the Supporting Information. This information is available free of charge via the Internet at http://pubs.acs.org.

Acknowledgements

Molecular simulations were performed using the Extreme Science and Engineering Discovery Environment (XSEDE), which is supported by National Science Foundation grant number ACI-1548562. Specifically, it used the Bridges system, which is supported by NSF award number ACI-1445606, at the Pittsburgh Supercomputing Center (PSC). This work also utilized the RMACC Summit supercomputer, which is supported by the National Science Foundation (awards ACI-1532235 and ACI-1532236), the University of Colorado Boulder, and Colorado State University. The Summit supercomputer is a joint effort of the University of Colorado Boulder and Colorado State University.

References

[1] H. Bekker, H. J. C. Berendsen, E. J. Dijkstra, S. Achterop, R. van Drunen, D. van der Spoel, A. Sijbers, H. Keegstra, B. Reitsma, and M. K. R. Renardus, "GROMACS: A Parallel Computer for Molecular Dynamics Simulations," in *Physics Computing '92 ed.*, World Scientific Publishing, 1993.

[2] H. J. C. Berendsen, D. van der Spoel, and R. van Drunen, "GROMACS: A Message-Passing Parallel Molecular Dynamics Implementation," *Comput. Phys. Commun.*, vol. 91, pp. 43–56, Sept. 1995.

[3] D. Van Der Spoel, E. Lindahl, B. Hess, G. Groenhof, A. E. Mark, and H. J. C. Berendsen, "GROMACS: Fast, Flexible, and Free," *J. Comput. Chem.*, vol. 26, pp. 1701–1718, Dec. 2005.

[4] B. Hess, C. Kutzner, D. van der Spoel, and E. Lindahl, "GROMACS 4: Algorithms for Highly Efficient, Load-Balanced, and Scalable Molecular Simulation," *J. Chem. Theory Comput.*, vol. 4, pp. 435–447, Mar. 2008.

[5] R. C. Smith, W. M. Fischer, and D. L. Gin, "Ordered Poly(p-phenylenevinylene) Matrix Nanocomposites via Lyotropic Liquid-Crystalline Monomers," *J. Am. Chem. Soc.*, vol. 119, no. 17, pp. 4092–4093, 1997.

[6] M. Zhou, P. R. Nemade, X. Lu, X. Zeng, E. S. Hatakeyama, R. D. Noble, and D. L. Gin, "New Type of Membrane Material for Water Desalination Based on a Cross-Linked Bicontinuous Cubic Lyotropic Liquid Crystal Assembly," *J. Am. Chem. Soc.*, vol. 129, pp. 9574–9575, Aug. 2007.

[7] R. Resel, U. Theissl, C. Gadermaier, E. Zojer, M. Kriechbaum, H. Amenitsch, D. Gin, R. Smith, and G. Leising, "The H2-Phase of the Lyotropic Liquid Crystal Sodium 3,4,5-Tris(omega-Acryloyloxyundecyloxy)benzoate," *Liq. Cryst.*, vol. 27, pp. 407–411, Mar. 2000.

[8] B. J. Coscia, J. Yelk, M. A. Glaser, D. L. Gin, X. Feng, and M. R. Shirts, "Understanding the Nanoscale Structure of Inverted Hexagonal Phase Lyotropic Liquid Crystal Polymer Membranes," *J. Phys. Chem. B*, vol. 123, pp. 289–309, Jan. 2019.

[9] J. Wang, R. M. Wolf, J. W. Caldwell, P. A. Kollman, and D. A. Case, "Development and Testing of a General Amber Force Field," *J. Comput. Chem.*, vol. 25, pp. 1157–1174, July 2004.

[10] J. Wang, W. Wang, P. A. Kollman, and D. A. Case, "Automatic Atom Type and Bond Type Perception in Molecular Mechanical Calculations," *J. Mol. Graphics. Modell.*, vol. 25, pp. 247–260, Oct. 2006.

[11] D. Case, R. Betz, W. Botello-Smith, D. Cerutti, T. Cheatham, III, T. Darden, R. Duke, T. Giese, H. Gohlke, A. Goetz, N. Homeyer, S. Izadi, P. Janowski, J. Kaus, A. Kovalenko, T. Lee, S. LeGrand, P. Li, C. Lin, T. Luchko, R. Luo, B. Madej, D. Mermelstein, K. Merz, G. Monard, H. Nguyen, H. Nguyen, I. Omelyan, A. Onufriev, D. Roe, A. Roitberg, C. Sagui, C. Simmerling, J. Swails, R. Walker, J. Wang, R. Wolf, X. Wu, L. Xiao, D. York, and P. Kollman, "AmberTools16," Apr. 2016.

[12] Y. Meroz and I. M. Sokolov, "A Toolbox for Determining Subdiffusive Mechanisms," *Physics Reports*, vol. 573, pp. 1–29, Apr. 2015.

[13] R. Metzler, J.-H. Jeon, A. G. Cherstvy, and E. Barkai, "Anomalous Diffusion Models and Their Properties: Non-Stationarity, Non-Ergodicity, and Ageing at the Centenary of Single Particle Tracking," *Phys. Chem. Chem. Phys.*, vol. 16, pp. 24128–24164, Oct. 2014.

[14] S. G. Schultz and A. K. Solomon, "Determination of the Effective Hydrodynamic Radii of Small Molecules by Viscometry," *The Journal of General Physiology*, vol. 44, pp. 1189–1199, July 1961.

[15] A. Luzar and D. Chandler, "Effect of Environment on Hydrogen Bond Dynamics in Liquid Water," *Phys. Rev. Lett.*, vol. 76, pp. 928–931, Feb. 1996.

[16] D. Prada-Gracia, R. Shevchuk, and F. Rao, "The quest for self-consistency in hydrogen bond definitions," *J. Chem. Phys.*, vol. 139, p. 084501, Aug. 2013.

[17] C. N. Rowley and B. Roux, "The Solvation Structure of Na+ and K+ in Liquid Water Determined from High Level ab Initio Molecular Dynamics Simulations," *J. Chem. Theory Comput.*, vol. 8, pp. 3526–3535, Oct. 2012.

[18] G. Srinivas, S. Bhattacharyya, and B. Bagchi, "Computer simulation and mode coupling theory study of the effects of specific solutesolvent interactions on diffusion: Crossover from a sub-slip to a super-stick limit of diffusion," *J. Chem. Phys.*, vol. 110, pp. 4477–4482, Feb. 1999.

TOC Graphic